Identification of time-dependent coefficients of heat transfer by the method of suboptimal stage-by-stage optimization

Article *in* International Journal of Heat and Mass Transfer · April 2013

DOI: 10.1016/j.ijheatmasstransfer.2012.12.029

2 authors, including:

Valentin Terent'evich Borukhov
National Academy of Sciences of Belarus

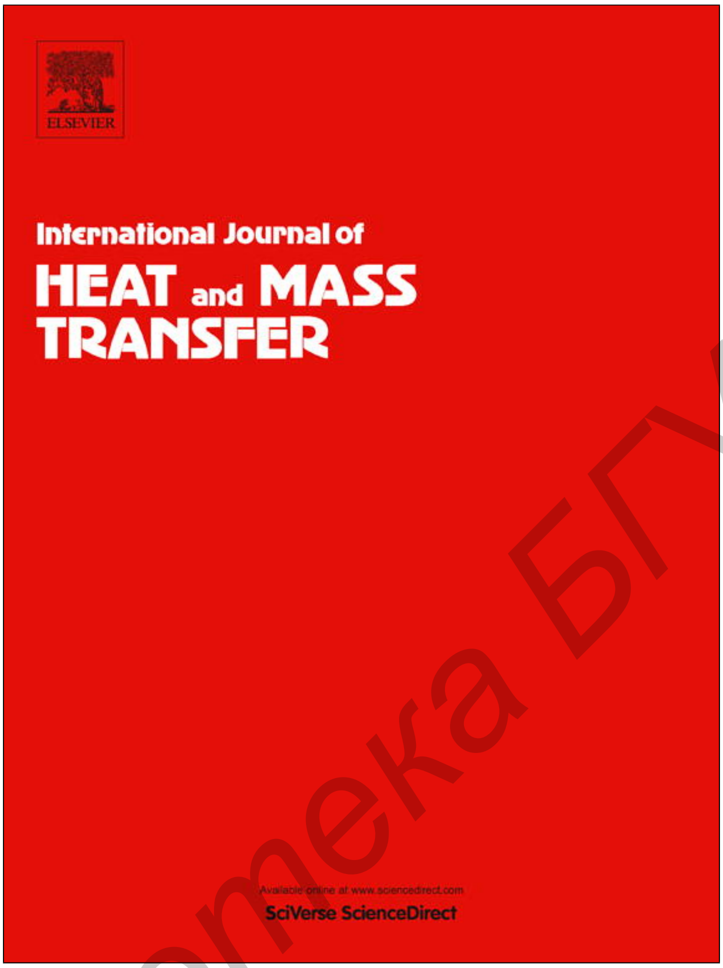
ELSEVIER
International Journal of
HEAT and MASS
TRANSFER
Available online at www.sciencedirect.com
SciVerse ScienceDirect

International Journal of Heat and Mass Transfer 59 (2013) 286–294

Contents lists available at SciVerse ScienceDirect

International Journal of Heat and Mass Transfer

journal homepage: www.elsevier.com/locate/ijhmt

Identification of time-dependent coefficients of heat transfer by the method of suboptimal stage-by-stage optimization

V.T. Borukhov, O.I. Kostyukova *

Institute of Mathematics, National Academy of Sciences of Belarus, Minsk 220072, Surganov Str. 11, Belarus

ARTICLE INFO

Article history:
Received 16 October 2012
Accepted 14 December 2012

Keywords:
Nonlinear heat conduction equation
Inverse problem
Stage-by-stage optimization
Heat transfer coefficient
Tikhonov regularization
Numerical simulation

ABSTRACT

An inverse heat conduction problem (IHCP) related to the recovery of time-dependent coefficients of heat transfer on the tube surface by the data of temperature measurement at two inner points of the tube is considered. Heat transfer is described by the initial boundary-value problem for 1D nonlinear heat conduction equation. To solve the posed IHCP a modified method of suboptimal stage-by-stage optimization (SSO) that allows one to process the input data in a real time mode is presented. Based on the computational experiment a conclusion is drawn that SSO possesses a regularization property in terms of A.N. Tikhonov.

1. Introduction

In investigation of heat transfer processes there arises a wide class of inverse heat conduction problems (IHCPs), viz., identification of coefficients, internal sources, boundary and initial conditions. In particular, for engineering and scientific applications the problem of recovery of time-dependent heat transfer coefficients by the data of temperature measurement at the inner points of the object [1–3].

As is known, IHCP refer to the class of ill-posed problems of mathematical physics. The fundamental concept of the regularization algorithm [4] forms the basis of modern computation procedures of IHCP solution. In this case, development of new approaches to the solution of IHCP is stimulated by a number of requirements among which we mention the following:

- stability of numerical algorithms of IHCP solution to small perturbations of the input data;
- use of the *a priori* information on the solution;
- effective implementation and high speed of numerical procedures of IHCP solution.

Extremal methods for solving ill-posed problems [2,4,5] correspond, to one or another degree, to the requirements mentioned above. In particular, in the theory and practice, the conjugate gradient method of residual functional minimization [2,5–7] is wide used for solving IHCP. For linear models of transfer, classical approaches [1,5] are developed that are based on the combination of the regularization technique and different notions of fundamental solutions [8]. The development of a new so-called Li-group shooting method for solving some classes of IHCP is presented in [9]. Recently, a Bayesian statistical inference method [10,11] is actively applied to solution of IHCP. We should mention also hybrid methods which combine algorithms of artificial neuron networks, genetic algorithms and procedures of annealing simulation [12,13].

An additional requirement

- data processing in a real time scale (the causality property)

arises in the problems of control over thermal processes.

For a number of problems of the recovery of internal sources and boundary regimes of heat transfer the methods of sequential function specification [1], semi-interval regularization [14], dynamic regularization [15,16], inverse dynamic systems [17–20] meet this requirement. In [21], a review of the regularization techniques that retain the causality property for solution of the first-kind Volterra equations is presented.

In the present paper we consider the problem of the recovery of heat transfer coefficients at the boundaries of the annular region. To solve this problem we develop the approach of suboptimal stage-by stage optimization (SSO) [22,23]. This approach belongs to the class of extremal methods of solution of ill-posed problems with specially selected regularization functionals.

* Corresponding author.
E-mail addresses: borukhov@im.bas-net.by (V.T. Borukhov), kostyukova@im.bas-net.by (O.I. Kostyukova).

0017-9310/$ - see front matter © 2012 Elsevier Ltd. All rights reserved.
http://dx.doi.org/10.1016/j.ijheatmasstransfer.2012.12.029

Nomenclature

A	thermal depth of thermocouple location
$C(T)$	heat capacity
g_σ^M	vector of input data
h	step of spatial grid
i_*	ill-posedness order
j	stage number
L_b	parameter determining the confidence interval $[\tau_j, \tau_j + L_b\Delta t]$
L	parameter characterizing the step length $L\Delta t$
$M + 1$	number of temperature measurements
N	dimensionality of the state vector of a finite-dimensional system
p	number of stages
r	coordinate
r_0	inner tube radius
r_*	outer tube radius
$r_1^*,\ r_2^*$	points of temperature measurement
$T = T(r,t)$	temperature field
$\overline{T}(r)$	initial temperature
$T_{fl}(t)$	temperature outside the tube
$T_{in}(t)$	temperature inside the tube
t	time
t_0	initial time instant
t_*	finite time instant
w_1, w_2	random variables
$U(t)$	control (heat flux)
u_σ^M	vector of output data

Greek symbols

α_1, α_2	heat transfer coefficients
α_1^*	estimate of the heat transfer coefficient α_1
β	aggregate regularization parameter
γ_j	penalty coefficient
$\lambda(T)$	thermal conductivity
$\rho(T)$	density
η_j	weighting coefficient of the Tikhonov regularizator
σ	standard deviation of the measurement error
Δt	step of the time grid

Subscripts and superscripts

i	index
j	index
k	index
s	index

Classical extremal regularization techniques do not allow data processing in the real (current) time scale since they involve conjugate problems that are solved in reverse time. An idea of the approach under development is rather simple (see, e.g., [1,14–16]). The total time segment is divided to parts (stages) compatible with the current time scale and at each step IHCP is solved by one of classical methods. In this case, the problem of joining the solutions at the points the junction of stages can arise for identification problems. Depending on the *a priori* information on the IHCP solution, this can be the requirement of continuous and rather smooth joining. These requirements are provided by an appropriate choice of penalty coefficients in the quality functional.

For nonlinear IHCP, the division to stages plays one more important role, since at each stage the system can be linearized, which at small length of the stage properly approximates the initial nonlinear system.

The SSO approach allows control of the vector of regularization parameters, which consists of

1. the ill-posedness order of the IHCP lumped model;
2. a set of weighting coefficients of Tikhonov regularizers;
3. a set of penalty coefficients that provide the continuity (smoothness) of the recovered function at the points of the stage-by-stage junction;
4. the stage length;
5. the step of discretization at a stage.

We note that using an appropriate set of the regularization vector components one can take into account the *a priori* information on the structure of the input data error, information on the portions of sought-for coefficient monotonicity, etc. The property of the SSO method to process the input data in a real time scale is due to reduction of the recovery problem to solving a simple small-dimension problem of square optimization at each stage. The same property allows one to use standard software MAPLE, Mathlab, etc.

The paper is organized as follows: introduction, three sections, conclusions, and appendix. In the first section the problem is formulated, in the second section the modified SSO method is stated in detail, in the third section we discuss the results of numerical simulation of the problem of identification of the heat transfer coefficient. Numerical simulation is aimed at experimental verification of the regularization property of the procedure proposed for IHCP solution. We note that parameters of the initial boundary-value problem considered at the beginning of the third section are borrowed from [24] where a mathematical model of ingots solidification in a jet crystallizer is presented. In the appendix, for convenience of the readers, we give the notion of the regularizing operator.

2. Problem formulation

Let an initial boundary-value problem for a nonlinear heat conduction equation be specified in the cylindrical system of coordinates

$$\rho(T)C(T)\frac{\partial T}{\partial t} = \frac{1}{r}\frac{\partial}{\partial r}\left(r\lambda(T)\frac{\partial T}{\partial r}\right),\ T = T(r,t),\ r_0 \leqslant r \leqslant r_*,\ t_0 \leqslant t \leqslant t_*, \tag{1}$$

$$-\lambda(T)\frac{\partial T}{\partial r}\bigg|_{r=r_0} = \alpha_1(t)(T_{in}(t) - T(r_0,t)), \quad t \in [t_0, t_*], \tag{2}$$

$$-\lambda(T)\frac{\partial T}{\partial r}\bigg|_{r=r_*} = \alpha_2(t)(T(r_*,t) - T_{fl}(t)), \quad t \in [t_0, t_*], \tag{3}$$

$$T(r,t_0) = \overline{T}(r), \quad r \in [r_0, r_*]. \tag{4}$$

The system of Eqs. (1)–(4) describes a nonstationary temperature field in a tube with outer radius $r_*$and inner radius r_0. In this case, the conditions of angular symmetry and independence of the temperature field of the axial coordinate are assumed to be met. Here $T = T(r,t),\ r \in [r_0, r_*] \subset \mathbb{R},\ t \in [t_0, t_*] \subset \mathbb{R}$ is the temperature distribution, $\alpha_1(t)$, $\alpha_2(t)$ are the heat transfer coefficients, $\lambda(T)$ is a heat-conductivity coefficient, $C(T)$ is the specific heat capacity of material. $\rho(T)$ is the material density, $T_{fl}(t)$ is the temperature of cooling liquid outside the tube, $T_{in}(t)$ is the temperature on the outer surface of the tube, and $\overline{T}(r)$ is the initial temperature of the tube.

We consider the problem of calculation of the heat transfer coefficients $\alpha_1(t)$, $\alpha_2(t)$, $t \in [t_0, t_*]$, on the basis of the known data

$$y_1(t) = T(r_1^*, t) + v_1(t), \quad y_2(t) = T(r_2^*, t) + v_2(t), \quad t \in [t_0, t_*], \tag{5}$$

on the values of temperature fields at two specified points $r_1^*,\ r_2^*,\ r_0 \leqslant r_1^* < r_2^* \leqslant r_*$.

Here the functions $v_1(t)$, $v_2(t)$ denote the measurement error. Following [1,2], in order to model the functions $v_1(\cdot)$, $v_2(\cdot)$ we use statistical description. With account for discrete presentation of measurements this description has the form

$$y_1(t_i) = T(r_1^*, t_i) + w_1\sigma, \quad i = 0, 1, \ldots, M; \tag{6}$$
$$y_2(t_i) = T(r_2^*, t_i) + w_2\sigma, \quad i = 0, 1, \ldots, M; \tag{7}$$

where

$$t_i = t_0 + i\Delta t, \quad \Delta t = (t_* - t_0)/M, \tag{8}$$

$\sigma$is the standard deviation of measurement errors, w_1 and w_2 are the random variables with normal distribution, zero-mean and unitary standard deviation.

Let the thermophysical parameters ρ, λ, and C, temperatures $T_{fl}(t)$, $T_{in}(t)$, $t \in [t_0, t_*]$, $\overline{T}(r)$, $r \in [r_0, r_*]$, and a value of error deviation σ be known. Then the general problem of identification of the heat transfer coefficients is in recovery of the functions $\alpha_1(t)$, $\alpha_2(t)$, $t \in [t_0, t_*]$, by the data (6), (7), and the system of Eqs. (1)–(4).

We note that the problem under consideration disintegrates to two subproblems which can be solved independently. The first subproblem is to determine the coefficient $\alpha_1(t)$, $t \in [t_0, t_*]$, by the data (6) and the system

$$\rho(T)C(T)\frac{\partial T}{\partial t} = \frac{1}{r}\frac{\partial}{\partial r}\left(r\lambda(T)\frac{\partial T}{\partial r}\right), \quad r_0 \leqslant r \leqslant r_2^*, \ t_0 \leqslant t \leqslant t_*, \tag{9}$$

$$-\lambda(T)\frac{\partial T}{\partial r}\bigg|_{r=r_0} = \alpha_1(t)(T_{in}(t) - T(r_0, t)), \quad T(r_2^*, t) = y_2(t), \ t \in [t_0, t_*], \tag{10}$$

$$T(r, t_0) = \overline{T}(r), \quad r \in [r_0, r_2^*]. \tag{11}$$

The second subproblem of the recovery of the coefficient $\alpha_2(t)$, $t \in [t_0, t_*]$, by the data (7) is determined similarly.

3. Approach of suboptimal optimization

We formulate the SSO method by an example of the problem recovery of the heat transfer coefficient by the data (6) and the system of Eqs. (9)–(11). We assume that the grid (8) is uniform, i.e., $t_i = t_0 + i\Delta t$, $i = 0, 1, \ldots, M$, $\Delta t = (t_* - t_0)/M$.

The essence of the method is in reduction of the problem of the coefficient $\alpha_1(t)$ recovery on the entire time interval $t \in [t_0, t_*]$ to successive solution of p problems of recovery of the coefficient $\alpha_1(t)$ on small time intervals $t \in [\tau_j, \tau_{j+1}]$, $j = 0, 1, \ldots, p-1$, where $\tau_j = t_0 + jL\Delta t$, and the integers $L > 0$, $p > 0$, $M > 0$ are related as $(p-1)L = M$. Here $L\Delta t$ is the length of the time interval determined by the parameter L and the quantity $\Delta t > 0$, which is the step of measurements in (6). The advantages of this approach will be stated below.

For a given j ($j = 0, \ldots, p-1$), in order to recover the coefficient $\alpha_1(t)$ at the jth stage $t \in [\tau_j, \tau_{j+1}]$ the following optimal control problem is solved.

Problem P_j: To find heat flux (a control) $U(t)$, $t \in [\tau_j, \tau_{j+1}]$, which minimizes the performance criterion

$$\sum_{i=jL+1}^{(j+1)L} \left(T(r_1^*, t_i) - y_1(t_i)\right)^2 + \eta_j \int_{\tau_j}^{\tau_{j+1}} \left(\frac{dU(t)}{dt}\right)^2 dt + \gamma_j (U^{(j-1)}(\tau_j - 0) - U(\tau_j + 0))^2 \to \min \tag{12}$$

on the trajectories $T(r, t)$, $r \in [r_0, r_2^*]$, $t \in [\tau_j, \tau_{j+1}]$, of the system

$$\rho(T)C(T)\frac{\partial T}{\partial t} = \frac{1}{r}\frac{\partial}{\partial r}\left(r\lambda(T)\frac{\partial T}{\partial r}\right), \quad r_0 \leqslant r \leqslant r_2^*, \ t \in [\tau_j, \tau_{j+1}], \tag{13}$$

$$-\lambda(T(r_0, t))\frac{\partial T(r_0, t)}{\partial r} = U(t); \quad T(r_2^*, t) = y_2(t), \ t \in [\tau_j, \tau_{j+1}], \tag{14}$$

$$T(r, \tau_j) = T^{(j-1)}(r, \tau_j - 0), \quad r \in [r_0, r_2^*]. \tag{15}$$

Here $\eta_j > 0$ is the weighting coefficient of the Tikhonov regularizer in the performance criterion (12), $\gamma_j > 0$ is the penalty coefficient for the term $\gamma_j(U^*(\tau_j - 0) - U(\tau_j + 0))^2$ in (12) which is responsible for junction of $U^{(j-1)}(\tau_j - 0)$ and $U^{(j)}(\tau_j + 0)$; $U^{(j-1)}(t)$, $T^{(j-1)}(r, t)$, $t \in [\tau_{j-1}, \tau_j]$, $r \in [r_0, r_2^*]$, are the optimal control and the corresponding temperature obtained at the previous $(j-1)$th stage. At $j = 0$ we assume that $\gamma_0 = 0$ and $T^{(j-1)}(r, \tau_0 - 0) = \overline{T}(r)$, $r \in [r_0, r_2^*]$.

Let $U^{(j)}(t)$ be the optimal control and $T^{(j)}(r, t)$, $t \in [\tau_j, \tau_{j+1}]$, $r \in [r_0, r_2^*]$, is the trajectory of the problem P_j correspondent to it. Then we assume

$$\alpha_1(t) \approx \alpha_1^*(t) := U^{(j)}(t)/(T_{in}(t) - T^{(j)}(r_0, t)), \quad t \in [\tau_j, \tau_{j+1}], \tag{16}$$

where $\alpha_1^*(t)$, $t \in [\tau_j, \tau_{j+1}]$, is an estimate of the coefficient $\alpha_1(t)$ at the jth stage.

To solve the problem P_j numerically, we approximate the nonlinear system of partial differential Eqs. (13)–(15) by a linear system of ordinary differential equations.

With this in mind we divide the interval $[r_0, r_2^*]$ to N parts by the points

$$r_i = r_0 + ih, \quad i = 0, 1, \ldots, N, \quad h = (r_2^* - r_0)/N, \quad r_1^* = r_{i_*} = r_0 + i_* h, \tag{17}$$

and denote $T(r_i, t) = T_i(t)$. Then the performance criterion (12) takes the form

$$\sum_{i=jL+1}^{(j+1)L} (T_{i_*}(t_i) - y_1(t_i))^2 + \eta_j \int_{\tau_j}^{\tau_{j+1}} \left(\frac{dU(t)}{dt}\right)^2 dt + \gamma_j (U^{(j-1)}(\tau_j - 0) - U(\tau_j + 0))^2 \to \min. \tag{18}$$

If N is rather large, then system (13)–(15) can be approximated by the nonlinear system of ordinary differential equations

$$\dot{T}_0(t) = \frac{\lambda(T_1(t))(T_1(t) - T_0(t))(1/r_0 + 1/h) + U^{(j)}(t)}{hc(T_0(t))\rho(T_0(t))}, \tag{19}$$

$$\dot{T}_i(t) = \frac{\lambda(T_i(t))(T_{i+1}(t) - T_i(t))(h/r_i + 1) - \lambda(T_{i-1}(t))(T_i(t) - T_{i-1}(t))}{h^2 c(T_i(t))\rho(T_i(t))}, \quad i = 1, 2, \ldots, N-2,$$

$$\dot{T}_{N-1}(t) = \frac{\lambda(T_{N-1}(t))(y_2(t) - T_{N-1}(t))(h/r_{N-1} + 1) - \lambda(T_{N-2}(t))(T_{N-1}(t) - T_{N-2}(t))}{h^2 c(T_{N-1}(t))\rho(T_{N-1}(t))}, \quad t \in [\tau_j, \tau_{j+1}],$$

with the initial conditions

$$T_i(\tau_j) = T_i^0(\tau_j) := T^{(j-1)}(r_i, \tau_j - 0), \quad i = 0, 1, \ldots, N-1. \tag{20}$$

Problems (18)–(20) is a problem of optimal control of the nonlinear dynamic system (19) with the N-dimensional vector of state $(T_0(t), T_1(t), \ldots, T_{N-1}(t))$ and scalar control $U(t)$, $t \in [\tau_j, \tau_{j+1}]$. It has a number of special features which do not allow use of standard computational packages designed for "standard" problems of optimal control. Therefore we make a series of simplifications.

First of all, on the interval $[\tau_j, \tau_{j+1}]$ we linearize system (19) having substituted it by the system of linear differential equations of the form

$$\dot{T}_0(t) = \frac{\lambda\left(T_1^0(\tau_j)\right)(T_1(t) - T_0(t))(1/r_0 + 1/h) + U^{(j)}(t)}{hc\left(T_0^0(\tau_j)\right)\rho\left(T_0^0(\tau_j)\right)}, \quad (21)$$

$$\dot{T}_i(t) = \frac{\lambda\left(T_i^0(\tau_j)\right)(T_{i+1}(t) - T_i(t))(h/r_i + 1) - \lambda\left(T_{i-1}^0(\tau_j)\right)(T_i(t) - T_{i-1}(t))}{h^2 c\left(T_i^0(\tau_j)\right)\rho(T_i^0(\tau_j))},$$
$$i = 1, 2, \ldots, N-2,$$

$$\dot{T}_{N-1}(t) = \frac{\lambda\left(T_{N-1}^0(\tau_j)\right)(y_2(t) - T_{N-1}(t))(h/r_{N-1} + 1) - \lambda\left(T_{N-2}^0(\tau_j)\right)(T_{N-1}(t) - T_{N-2}(t))}{h^2 c\left(T_{N-1}^0(\tau_j)\right)\rho\left(T_{N-1}^0(\tau_j)\right)},$$

with the initial conditions (20). We recall that here the data $T_0^0(\tau_j), T_1^0(\tau_j), \ldots, T_{N-1}^0(\tau_j)$ are determined according to (20), i.e., they are known at the time instant τ_j.

Moreover, we solve this problem in the class of piecewise constant admissible control

$$U(t) = U_i = const, \quad t \in [t_i, t_{i+1}], \quad i = jL, \ldots, (j+1)L - 1. \quad (22)$$

The problem (18), (20)–(22) is easily reduced (see, e.g., [23]) to a problem of quadratic programming and can be solved by standard techniques. Let $U(t) = U^{(j)}(t)$, $t \in [\tau_j, \tau_{j+1}]$, be the optimal control of the linear-quadratic problem (18), (20)–(22). Using this control, we integrate the system of nonlinear partial differential Eqs. (13)–(15) and obtain the corresponding trajectory

$$T^{(j)}(r,t), \quad r \in [r_0, r_*], \quad t \in [\tau_j, \tau_{j+1}]. \quad (23)$$

Knowing trajectory (23), we calculate the coefficient $\alpha_1^*(t), t \in [\tau_j, \tau_{j+1}]$, by formula (16) and find the initial conditions

$$T^{(j)}(r, \tau_{j+1} - 0), \; r \in [r_0, r_2^*],$$

for the following $(j+1)$ th stage (for the following problem P_{j+1}).

Thus, in the technique suggested the solution of one problem of recovery for linear system (9) and (10) on a "large" interval $t \in [t_0, t_*]$ is reduced to successive solution of the problems of optimal control (18), (20)–(22) by linear systems on each "small" interval $t \in [\tau_j, \tau_{j+1}]$, $j = 0, \ldots, p-1$.

We note that in the one-stage ($p = 1$) procedure of recovery one problem of optimal control is solved on the entire interval $[t_0, t_*]$. In this case, its dimensions increase with decrease of steps Δt and h, which makes impossible solution of the problem at high accuracy of approximation.

In the approach suggested at any choice of arbitrary small values of steps Δt and h the dimensions of quadratic programming problems, which are solved at the stages, can be arbitrary *a priori* specified (only the number of stages can increase).

Moreover, at each stage the results of recovery can be analyzed, and using the results of the analysis the regularization parameters can be corrected.

It is seen from the given description of the SSO method that its implementation is related to the solution of optimal control problems (18), (20)–(22) on each interval $[\tau_j, \tau_{j+1}]$, $j = 0, \ldots, p-1$. Since each of these problems is reduced to the corresponding quadratic programming problem of small dimensionality, all these problems are solved by standard methods. In particular, for both solution of quadratic programming problems and integration of the systems of differential equations we used the mathematic package MATLAB 7.0.

For the optimal control problems (18), (20)–(22) of great importance is the value of the index i_*, that is determined by the parameters r_1^* and N (see relation (17)). The value of the index i_* is equal to the index k of the performance criterion of the problem. We recall [23,25] that the index of the performance criterion

$$\int_a^b f(T_s(t), s = 0, \ldots, N-1, U(t))dt$$

is the smallest integer number k, at which

$$\frac{\partial}{\partial U}\frac{d^k}{dt^k} f(T_s(t), s = 0, \ldots, N-1, U(t)) \neq 0.$$

Here the derivatives

$$\frac{d^k}{dt^k} T_s(t), \quad s = 0, \ldots, N-1,$$

are calculated with account for the specified system of differential equations. In the case under consideration this is system (21).

The value of the index k characterizes the degree of direct influence of control $U(t)$, $t \in [t_0, t_*]$, on the performance criterion. The higher the value of k the weaker the influence of $U(t)$, $t \in [t_0, t_*]$, on the performance criterion (more exactly on the first term of it which is responsible for the quality of recovery) and the more 'irregular' the recovery problems become. Therefore, in what follows we call the quantity $i_* = k$ the order of ill-posedness of the lumped model (18)–(20) of the problem of recovery of the coefficient. We note that $i_* = (r_1^* - r_0)/h$.

An analysis of problem (18), (20)–(22) shows that the weakest influence on the first term

$$\sum_{i=jL+1}^{(j+1)L} (T_{i_*}(t_i) - y_1(t_i))^2$$

in criterion (18) is exerted by the values of the control $U(t) = U^{(j)}(t)$, $t \in [\tau_j, \tau_{j+1}]$, that are the closest to the end of the interval $[\tau_j, \tau_{j+1}]$ (the closer to the end of the interval, the weakest the influence). These control values are selected mainly in order to minimize the regularization term

$$\int_{\tau_j}^{\tau_{j+1}} \left(\frac{dU(t)}{dt}\right)^2 dt$$

in criterion (18). It is obvious that values of these control values will be 'regular', but far from those under recovery.

In order to overcome the difficulties that arise at a large value of the index i_*, the above-described algorithm should be altered as follows.

One more parameter L_b, $0 \leqslant L_b \leqslant L$, is selected. It is assumed that the integer L_b is such that the number $(t_* - t_0)/L_b$ is integer. The parameter L_b defines that part of the interval (the confidence interval) $[\tau_j, \tau_j + L_b\Delta t]$, where the obtained control values

$$U^{(j)}(t), t \in [\tau_j, \tau_j + L_b\Delta t] \subset [\tau_j, \tau_{j+1} = \tau_j + L\Delta t],$$

are taken to be recovered. Only this part $U^{(j)}(t)$, $t \in [\tau_j, \tau_j + L_b\Delta t]$, of the obtained control $U^{(j)}(t)$, $t \in [\tau_j, \tau_j + L\Delta t]$, is used at subsequent calculations.

With account for the alterations made the algorithm takes the following form:

Step 0. We have the initial data $j = 0$, $\bar{\tau}_0 = t_0$, $T^{(-1)}(r, \bar{\tau}_0) = \overline{T}(r)$, $r \in [r_0, r_*]$, $x_i^0(t)$, $t \in [t_0, t_*]$, $i = 1, 2$.

Step 1. We assume $T_0^0(\bar{\tau}_j) = T^{(j-1)}(r_0, \bar{\tau}_j), T_1^0(\bar{\tau}_j) = T^{(j-1)}(r^1, \bar{\tau}_j), \ldots, T_{N-1}^0(\bar{\tau}_j) = T^{(j-1)}(r^{N-1}, \bar{\tau}_j)$. We solve the optimal control problem (18), (20)–(22) on the interval $[\bar{\tau}_j, \tau_{j+1}^*]$, where $\tau_{j+1}^* = \min\{\bar{\tau}_j + L\Delta t, t_*\}$. We obtain optimal control $U^{(j)}(t), t \in [\bar{\tau}_j, \tau_{j+1}^*]$.

Step 2. We assume $\bar{\tau}_{j+1} := \bar{\tau}_j + L_b\Delta t$ and on the interval $[\bar{\tau}_j, \bar{\tau}_{j+1}] \subset [\bar{\tau}_j, \tau_{j+1}^*]$ we integrate the nonlinear system of partial differential Eqs. (13)–(15) with the found control

$U^{(j)}(t),\ t \in [\bar{\tau}_j, \bar{\tau}_{j+1}]$, and obtain the trajectory $T^{(j)}(r,t),\ r \in [r_0, r_2^*],\ t \in [\bar{\tau}_j, \bar{\tau}_{j+1}]$.
Step 3. We find the coefficient $\alpha_1^*(t),\ t \in [\bar{\tau}_j, \bar{\tau}_{j+1}]$, from relations (16).
Step 4. If $\bar{\tau}_{j+1} = t_*$, we go to Step 6, otherwise to Step 5.
Step 5. We set $j := j+1$ and go to Step 1.
Step 6. Stop of the algorithm. The constructed function $\alpha_1^*(t)$, $t \in [t_0, t_*]$, is taken as the recovered coefficient of heat transfer.

The procedure mentioned is in agreement with the approach of successive regularization [1,14].

4. Numerical simulation

Since application of regularizing algorithms (see Appendix) allows obtaining physically admissible, stable to disturbances of input data, solutions of inverse problems, it is important to prove the regularizability property of the SSO algorithm. However, in the general case, a mathematically rigorous proof of this property has not been obtained as yet. Therefore, numerical simulation of the SSO approach is of importance.

We denote

$$u_\sigma(t_i) = \alpha_1^*(t_i), \quad y_\sigma(t_i) = y_1(t_i), \quad i = 0, 1, \ldots, M,$$

where the subscript σ indicates, according to (6) the dependence of data $\alpha_1^*(t_i),\ y_1(t_i)$ on the random variable w_1. We present the dependence of the vector of output data

$$u_\sigma^M = [u_\sigma(t_1), \ldots, u_\sigma(t_M)] \tag{24}$$

of the SSO algorithm on the vector of input data

$$y_\sigma^M = [y_\sigma(t_1), \ldots, y_\sigma(t_M)] \tag{25}$$

in the form

$$u_\sigma^M = R_\beta(y_\sigma^M), \tag{26}$$

where

$$\beta = \frac{1}{i_*} + \Delta t + \max_{j=0,\ldots,p-1}\{\eta_j\} + \max_{j=0,\ldots,p-1}\{\gamma_j\}$$

is the aggregate regularization parameter, i_* is the order of ill-posedness of the lumped model (18)–(20) of the initial boundary-value problem (13)–(15) with the performance criterion (12), η_j is the weighting coefficient of the Tikhonov regularizer in (12), γ_j is the penalty coefficient for the term in (12) which is responsible for junction, and Δt is the step of the time grid. The parameter Δt determines the so-called step regularization [1,5] of the algorithm.

With account for the definition of the regularizing algorithm (see Appendix A), the hypothetical assertion on the presence of the regularizability property of the SSO algorithm can be formulated as follows.

Assertion 1. There exists a dependence $\beta(\sigma)$ such that if the time step of measurements and the value of measurement error deviation σ tend to zero, then the output data (24) of the algorithm tend to exact values of the heat transfer coefficient.

Here we do not specify in which sense one should consider the convergence of data (24) to exact values (point-by-point convergence, mean convergence, etc.), since this is a subject of additional investigations.

Two series of numerical simulation of the problem of recovery of the coefficient α_1, assuming that thermophysical parameters are constant, were conducted. In this case, we considered two classes of problems: 'good' problems for which the thermal depth $A = (r_1^* - r_0)\sqrt{\rho C/\lambda}$ of thermocouple location satisfies the condition $A < 2$ and 'bad' problems when $A \gg 2$. The numerical experiment results presented in what follows indicate that the SSO algorithm possesses the regularizability property.

4.1. Numerical experiment. Recovery by the noised data

To verify the efficiency of the method suggested we conducted two series of numerical experiments.

First, we considered system (9)–(11) with the following values of the parameters ('good' problem)

$$C = 1085\ \mathrm{J/(kg\,K)}, \quad \rho = 2500\ \mathrm{kg/m^3}, \quad \lambda = 104\ \mathrm{W/(m\,K)}, \tag{27}$$

$$t_0 = 5\ \mathrm{s}, \quad t_* = 100\ \mathrm{s}, \quad r_0 = 0.0375\ \mathrm{m}, \quad r_* = r_2^* = 0.0475\ \mathrm{m}. \tag{28}$$

The functions $y_2(t)$ and $T_{in}(t)$, $t \in [t_0, t_*]$, are presented in Figs. 1 and 2, respectively, $\overline{T}(r) = -3910r + 285.065,\ r \in [r_0, r_*]$.

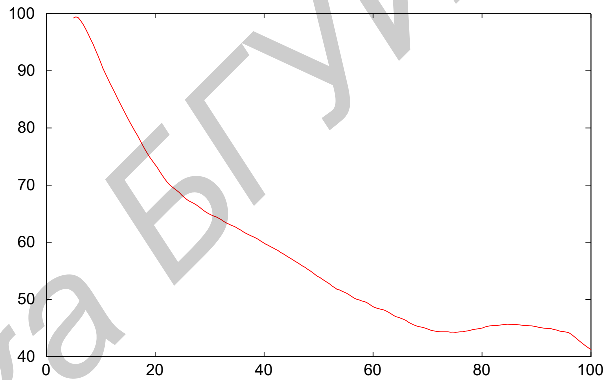

Fig. 1. Function $y_2(t)$, $t \in [t_0, t_*]$ in the first series of the experiments.

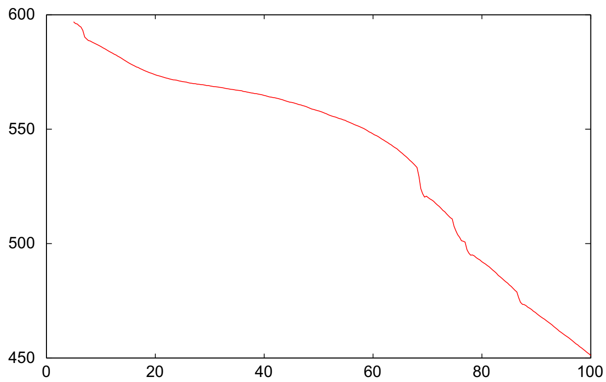

Fig. 2. Function $T_{in}(t)$, $t \in [t_0, t_*]$.

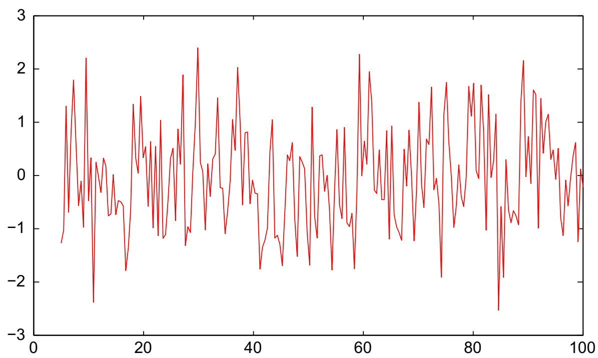

Fig. 3. Example of implementation of the function $w_1(t)$, $t \in [t_0, t_*]$.

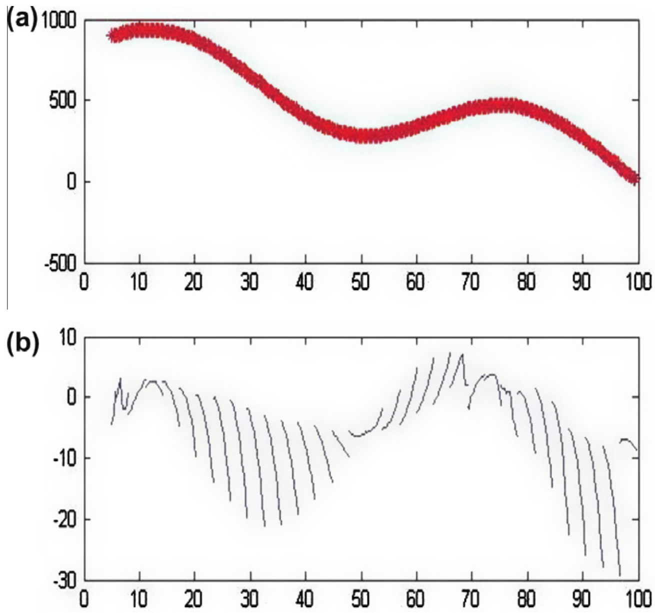

Fig. 4. Results of the numerical experiment at $N = 21$, $M = 312$, $i_* = 20$, $L = 20$, $L_b = 10$, $\eta_j = 0.000167$, $\gamma_j = 0.000067$, $\sigma = 0$: (a) solid line denotes the model heat transfer coefficient $\alpha_1(t)$, $t \in [t_0, t_*]$; bold line denotes the recovered heat transfer coefficient $\alpha_1^*(t)$, $t \in [t_0, t_*]$; (b) deviation $\Delta(t) = \alpha_1(t) - \alpha_1^*(t)$, $t \in [t_0, t_*]$.

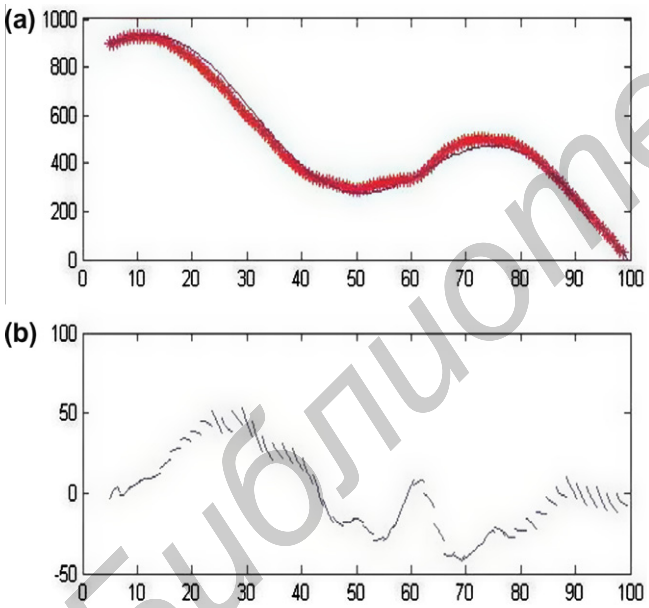

Fig. 5. Results of the numerical experiment at $N = 21$, $M = 155$, $i_* = 20$, $L = 30$, $L_b = 3$, $\eta_j = \gamma_j = 0.00033$, $\sigma = 0.3$: (a) solid line denotes the model heat transfer coefficient $\alpha_1(t)$, $t \in [t_0, t_*]$; bold line denotes the recovered heat transfer coefficient $\alpha_1^*(t)$, $t \in [t_0, t_*]$; (b) deviation $\Delta(t) = \alpha_1(t) - \alpha_1^*(t)$, $t \in [t_0, t_*]$.

Thermophysical parameters (27) correspond to the material of the casing of a jet crystallizer for solidification of ingots [24].

As the model coefficient under recovery $\alpha_1(t)$, $t \in [t_0, t_*]$, we took the function

$$\alpha_1(t) = 140(5 - t)/19 + 800 + 200 sin(t/10), \quad t \in [t_0, t_*]. \tag{29}$$

To obtain the noised measurement data (6) at a given point $r_1^* \in [r_0, r_*]$, we integrated system (9)–(11) with the above-indicated data and assumed

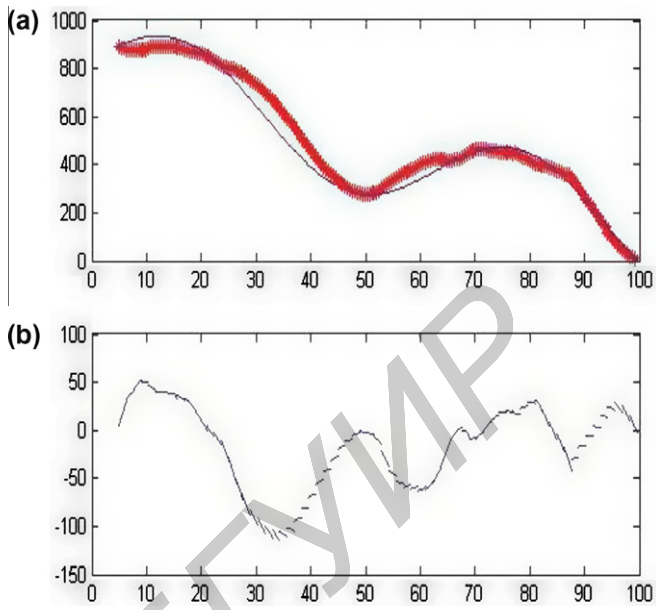

Fig. 6. Results of the numerical experiment at $N = 21$, $M = 235$, $i_* = 20$, $L = 30$, $L_b = 3$, $\eta_j = \gamma_j = 0.00167$, $\sigma = 1$: (a) solid line denotes the model heat transfer coefficient $\alpha_1(t)$, $t \in [t_0, t_*]$; bold line denotes the recovered heat transfer coefficient $\alpha_1^*(t)$, $t \in [t_0, t_*]$; (b) deviation $\Delta(t) = \alpha_1(t) - \alpha_1^*(t)$, $t \in [t_0, t_*]$.

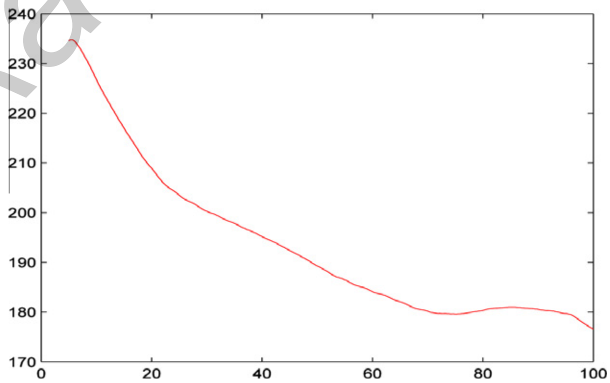

Fig. 7. Function $y_2(t)$, $t \in [t_0, t_*]$ in the second series of the experiments.

$$y_1(t) := T(r_1^*, t) + w_1(t)\sigma, \ t \in [t_0, t_*], \tag{30}$$

where σ is the standard quantity of measurement error deviation, $w_1(t)$ is a random variable with normal distribution, zero, mean, and unitary standard deviation. An example of implementation of the function $w_1(t)$, $t \in [t_0, t_*]$, is given in Fig. 3.

Then we solved the problem of recovery of the heat transfer coefficient $\alpha_1(t)$, $t \in [t_0, t_*]$, by data (30) and system (9) and (10) with the known functions $T_{in}(t)$, $y_2(t)$, $t \in [t_0, t_*]$, $\overline{T}(r)$, $r \in [r_0, r_*]$, and parameters (27) and (28).

For the considered series of 'good' problems we have $A = \sqrt{2.61} = 1.615 < 2$. Results of the numerical experiment are presented in Figs. 4–6 for $N = 21$, the value of the point $r_1^* = 0.047 \in [r_0, r_*]$ (i.e., value $i_* = 20$) where measurements are made, and different values of σ that characterize the level of noise, and also different values of the regularization parameters M, L, L_b, η_j, γ_j. We note that for $N = 21$, $i_* = 20$ we have $A = 1.53 < 2$.

In Figs. 4–6, graph (a) illustrates the model heat transfer coefficient $\alpha_1(t)$, $t \in [t_0, t_*]$, (see (29)) and the recovered coefficient $\alpha_1^*(t)$, $t \in [t_0, t_*]$. Graph (b) shows the deviation function $\Delta(t) = \alpha_1(t) - \alpha_1^*(t)$, $t \in [t_0, t_*]$.

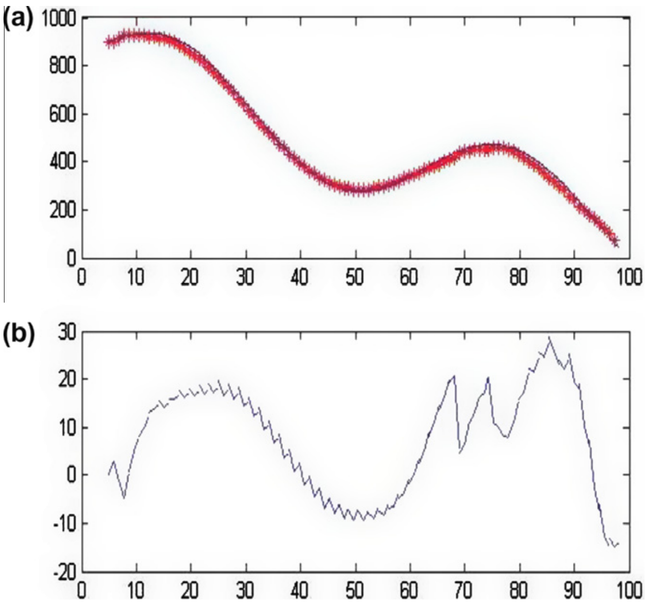

Fig. 8. Results of the numerical experiment at $N = 21$, $M = 105$, $i_* = 5$, $L = 30$, $L_b = 2$, $\eta_j = 0.0005/3$, $\gamma_j = 0.005/3$, $\sigma = 0$: (a) solid line denotes the model heat transfer coefficient $\alpha_1(t)$, $t \in [t_0, t_*]$; bold line denotes the recovered heat transfer coefficient $\alpha_1^*(t),\ t \in [t_0, t_*]$; (b) deviation $\Delta(t) = \alpha_1(t) - \alpha_1^*(t),\ t \in [t_0, t_*]$.

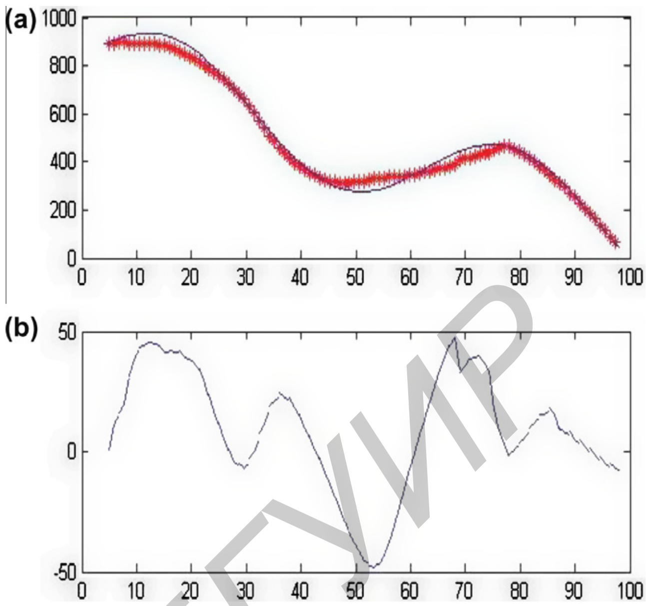

Fig. 10. Results of the numerical experiment at $N = 21$, $M = 105$, $i_* = 5$, $L = 30$, $L_b = 2$, $\eta_j = 0.005/3$, $\gamma_j = 0.05/3$, $\sigma = 1$: (a) solid line denotes the model heat transfer coefficient $\alpha_1(t)$, $t \in [t_0, t_*]$; bold line denotes the recovered heat transfer coefficient $\alpha_1^*(t),\ t \in [t_0, t_*]$; (b) deviation $\Delta(t) = \alpha_1(t) - \alpha_1^*(t),\ t \in [t_0, t_*]$.

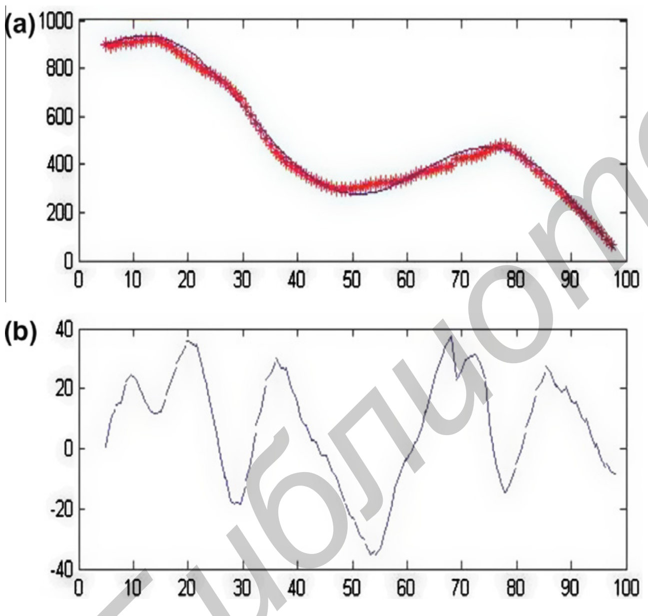

Fig. 9. Results of the numerical experiment at $N = 21$, $M = 105$, $i_* = 5$, $L = 30$, $L_b = 2$, $\eta_j = 0.001/3$, $\gamma_j = 0.01/3$, $\sigma = 0.5$: (a) solid line denotes the model heat transfer coefficient $\alpha_1(t)$, $t \in [t_0, t_*]$; bold line denotes the recovered heat transfer coefficient $\alpha_1^*(t),\ t \in [t_0, t_*]$; (b) deviation $\Delta(t) = \alpha_1(t) - \alpha_1^*(t), t \in [t_0, t_*]$.

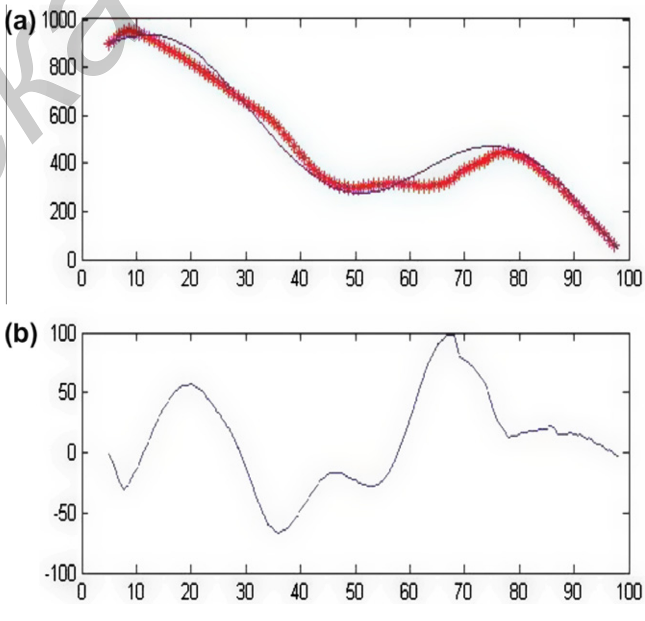

Fig. 11. Results of the numerical experiment at $N = 21$, $M = 105$, $i_* = 18$, $L = 30$, $L_b = 2$, $\eta_j = 0.00001$, $\gamma_j = 0.0001$, $\sigma = 0$: (a) solid line denotes the model heat transfer coefficient $\alpha_1(t)$, $t \in [t_0, t_*]$; bold line denotes the recovered heat transfer coefficient $\alpha_1^*(t),\ t \in [t_0, t_*]$; (b) deviation $\Delta(t) = \alpha_1(t) - \alpha_1^*(t),\ t \in [t_0, t_*]$.

We conducted the second series of experiments for the case of a thermally thick tube in a similar manner. The length of the interval $[r_0, r_*]$ was 10 times longer, i.e., parameters (28) were replaced by the following parameters:

$$r_0 = 0.375, \quad r_* = 0.475. \tag{31}$$

Values of parameters (27) and the function $T_{in}(t)$, $t \in [t_0, t_*]$, were conserved. As the function $y_2(t)$, $t \in [t_0, t_*]$, we took the function given in Fig. 7. The function $\overline{T}(r), r \in [r_0, r_*]$, was assumed equal to $\overline{T}(r) = -1676.7r + 1031.022,\ r \in [r_0, r_*]$.

As the model recovered coefficient $\alpha_1(t)$, $t \in [t_0, t_*]$, as previously, we took function (29).

Substitution of data (28) by (31) substantially complicates the problem of recovery of the heat transfer coefficient since now $A = \sqrt{261} \gg 2$.

The results of the second series of the numerical experiment are presented in Figs. 8–13 for $N = 21$, $M = 105$, $L = 30$, $L_b = 2$ and different values of points $r_1^* \in [r_0, r_*]$ (i.e., for different values of $i_* \in \{1, \ldots, N\}$), different values of σ, and different values of the parameters η_j, γ_j. We note that at $N = 21$, $i_* = 5$ we have $A = 3.23 > 2$ and at $N = 21$, $i_* = 18$ we have $A = 13.7 > 2$.

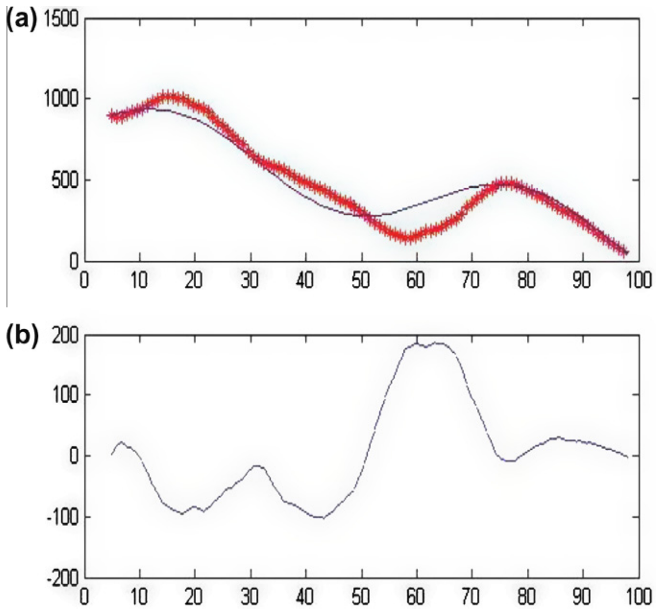

Fig. 12. Results of the numerical experiment at $N = 21$, $M = 105$, $i_* = 18$, $L = 30$, $L_b = 2$, $\eta_j = 0.0001$, $\gamma_j = 0.001$, $\sigma = 0.5$: (a) solid line denotes the model heat transfer coefficient $\alpha_1(t)$, $t \in [t_0, t_*]$; bold line denotes the recovered heat transfer coefficient $\alpha_1^*(t)$, $t \in [t_0, t_*]$; (b) deviation $\Delta(t) = \alpha_1(t) - \alpha_1^*(t)$, $t \in [t_0, t_*]$.

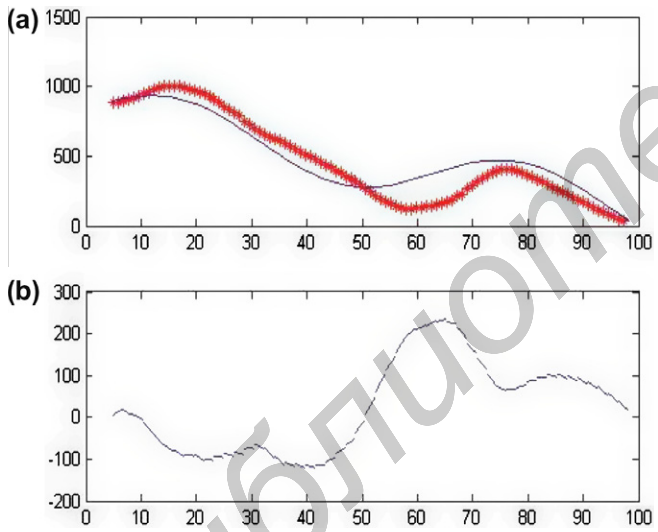

Fig. 13. Results of the numerical experiment at $N = 21$, $M = 105$, $i_* = 18$, $L = 30$, $L_b = 2$, $\eta_j = 0.0005/3$, $\gamma_j = 0.001/3$, $\sigma = 1$: (a) solid line denotes the model heat transfer coefficient $\alpha_1(t)$, $t \in [t_0, t_*]$; bold line denotes the recovered heat transfer coefficient $\alpha_1^*(t)$, $t \in [t_0, t_*]$; (b) deviation $\Delta(t) = \alpha_1(t) - \alpha_1^*(t)$, $t \in [t_0, t_*]$.

As in the previous series, in Figs. 8–13 graph (a) illustrates the model heat transfer coefficient $\alpha_1(t)$, $t \in [t_0, t_*]$, (see (29)) and the recovered coefficient $\alpha_1^*(t)$, $t \in [t_0, t_*]$. Graph (b) shows the differencing function $\Delta(t) = \alpha_1(t) - \alpha_1^*(t), t \in [t_0, t_*]$.

5. Conclusions

We suggested a modified SSO approach to recovery of time-dependent heat transfer coefficients in the initial boundary-value problem for a nonlinear heat conduction equation in the cylindrical system of coordinates. The SSO approach develops the method of Tikhonov regularization of ill-posed problems with account for the requirement of data processing in a real time scale.

It follows from the numerical experiment that the SSO algorithm possesses regularizing properties. In particular, with the aid of the SSO algorithm, depending on the level of noise, the heat transfer coefficient is recovered for a wide range of thermal depths of thermocouple location.

Appendix A

We consider the problem

$$Az = f, \quad z \in Z, \quad f \in F, \tag{32}$$

where f is a vector of exact input data, z is a sought-for solution of the problem, Z and F are metric spaces, and A is continuous, in the general case, nonlinear operator. In practice, the input data are specified inaccurately, therefore, instead of (32) one should consider the problem of search of an approximate solution z_δ from the equation

$$Az_\delta = f_\delta,$$

where the vector f_δ of disturbed input data satisfies the condition $\rho(f,f_\delta) \leqslant \delta$, δ is an estimate of input data error, and ρ is a metric in the space F.

Problem (32) is well-posed according to Hadamard if in some δ_0- neighbourhood $Q_f = \{g|\rho(f,g) < \delta_0\}(\delta_0 \geqslant \delta)$ of the vector f there exists continuous inverse operator A^{-1}. If the inverse operator is not determined on Q_f or is discontinuous, then problem (32) is ill-posed.

Solution of the well-posed problem (32) in the case of inaccurately specified input data can be presented in the form

$$z_\delta = A^{-1} f_\delta. \tag{33}$$

We can also take, as an approximate solution z_δ, an arbitrary vector from the set

$$Z_\delta = \{g|\rho(Ag, f_\delta) \leqslant \delta\}.$$

In this case, by virtue of A^{-1} continuity, the stability (well-posedness) requirement

$$\lim_{\delta \to 0} \rho(z_\delta, z) = 0 \tag{34}$$

of the problem will be met.

For ill-posed problem the solution of the form (33) does not any more satisfy condition (34) with an appropriate choice of a set of the vectors f_δ. From the physical point of view this indicates the absence of the reasonable interpretation of solution (33). On the other hand, for a large class of ill-posed problems there exists the possibility of selection of admissible solutions [4]. Namely, approximate solutions of the type $z_\beta = R_\beta(f_\delta)$, where R_β is a regularizing operator, satisfy the stability property (34). In this case, the operator R_β is called regularizing [4,26] if:

(1) it is determined on the set $\{g|\rho(f,g) \leqslant \delta\}$ for any β(the regularization parameter) from the semi-interval $(0, \beta_0]$, where β_0 is some positive number;
(2) there exists the dependence $\beta(\delta)$ such that the stability condition (34) is met when z_δ is selected in the form $z_\delta = R_\beta(f_\delta)$.

Physically, the interpreted solutions of ill-posed problems can be obtained by numerical algorithms that approximate the regularizing operator. Extensive physical and mathematical literature (see, e.g., review [26]) is devoted to a proof of this assertion for different schemes of approximation. The thus-obtained algorithms are also called regularizing.

References

[1] J.V. Beck, B. Blackwell, C.R. Clair, Inverse Heat Conduction: Ill-Posed Problems, Wiley-Interscince, New York, 1985.

[2] M.N. Ozisik, H.R.B. Orlande, Inverse Heat Transfer: Fundamentals and Applications, Tailor and Francis, New York, 2000.

[3] X.T. Xiong, X.H. Liu, Y.M. Yan, H.B. Guo, A numerical method for identifying heat transfer coefficient, Appl. Math. Model. 34 (2010) 1930–1938.

[4] A.N. Tikhonov, E.A. Arsenin, Solution of Ill-Posed Problems, Winston & Sons, Washington, DC, 1977.

[5] O.M. Alifanov, Inverse Heat Transfer Problems, Springer-Verlag, Berlin, 1994.

[6] J. Su, A.J. Silva Neto, Heat source estimation with the conjugate gradient method in inverse linear diffusive problems, J. Braz. Soc. Mech. Sci. 23 (2001) 321–334.

[7] V.T. Borukhov, V.A. Tsurko, G.M. Zayats, The functional identification approach for numerical reconstruction of the temperature dependent thermal conductivity coefficient, Int. J. Heat Mass Transfer 52 (2009) 232–238.

[8] M. Mierzwiezak, J.A. Kolodziej, The determination of heat source two dimensional inverse steady heat problems by means of the method of fundamental solutions, Inverse Probl. Sci. Eng. 19 (6) (2011) 777–792.

[9] C.-S. Liu, A self-adaptive LGSM to recover initial condition or heat source of one-dimensional heat conduction equation by using only minimal boundary thermal data, Int. J. Heat Mass Transfer 54 (2011) 1305–1312.

[10] C. Lieberman, K. Willcox, O. Chattas, Parameter and state model reduction for large-scale statistical inverse problems, SIAM J. Sci. Comput. 32 (6) (2010) 2523–2542.

[11] J. Wang, N. Zabaras, A Bayesian Inference approach to the inverse heat conduction problem, Int. J. Heat Mass Transfer 47 (2004) 3927–3941.

[12] A.J. Silva Neto Jr., J. Lugon, F.J.C.P. Soeiro, L.Biondi Neto, C.C. Santana, F.S. Lobato, V.S. Junior, Application of simulated annealing and hybrid methods in the solution of inverse heat and mass transfer problems, in: Rui Chibante (Ed.), Simulated Annealing, Theory and Application, Seiyo, 2010.

[13] V.C. Mariani, L. dos Santos Coelho, Global optimization of thermal conductivity using stochastic algorithms, Inverse Probl. Sci. Eng. 47 (4) (2009) 511–535.

[14] O.M. Alifanov, Identification of Processes of Heat Container Apparatus, An Introduction to the Theory of Inverse Problem of Heat Transfer, Machinery Pyblisher, Moscow 1979 (in Russian).

[15] A.I. Korotkii, Inverse problems of the dynamics of control system with distributed parameters, Russ. Math. N 11 (1995) 101–124.

[16] V.I. Maksimov, Method of controlled models in the problem of reconstructing a boundary input, Proc. Steklov Inst. Math. 262 (2008) 178–186.

[17] V.T. Borukhov, Reconstruction of heat fluxes though differential temperature measurement by the method of inverse dynamical systems, J. Eng. Phys. Thermophys. 47 (1984) 1098–1102.

[18] V.T. Borukhov, P.M. Kolesnikov, Method of inverse dynamic systems and its application for recovering internal heat sources, Int. J. Heat Mass Transfer 31 (1988) 1549–1556.

[19] V.T. Borukhov, P.N. Vabishchevich, Numerical solution of the inverse problem of reconstructing a distributed right-hand side of parabolic equation, Comput. Phys. Commun. 126 (1–2) (2000) 32–36.

[20] E.A. Kalinina, Numerical study of inverse problem of identification of source density for two-dimensional non-stationary convention–diffusion equation, Far Eastern Math. J. 5 (2004) 89–99 (in Russian).

[21] P.L. Lamm, A survey of regularization methods for first-kind Volterra equations, in: D. Colton, H.W. Engl, A. Loieis, J.R. McLanghin, W. Rundell (Eds.), Surveys on Solution Methods for Inverse Problems, Springer, Vienna, New York, 2000, pp. 53–82.

[22] K. Eppler, F. Troltzsch, Fast solution of optimal control problems in the selective cooling of steel, ZAMM 81 (2001) 447–456.

[23] V.T. Borukhov, O.I. Kostyukova, M.A. Kurdina, Tracking of the preset program of weighted temperatures and reconstruction of heat transfer coefficients, J. Eng. Phys. Thermophys. 83 (2010) 622–631.

[24] V.T. Borukhov, G.M. Zayats, V.Yu. Stetsenko, R.V. Kovalnogov, Determination of heat transfer coefficients during solidification of a casting in a jet crystallizer, J. Eng. Phys. Thermophys. 85 (2012) 195–202.

[25] K. Malanowski, H. Maurer, Sensitivity analysis of optimal control problems subject to higher order state constraints, Ann. Oper. Res. (Optim. Data Perturb. II) 101 (2001) 43–73.

[26] O.A. Liskovets, Theory and methods of solving ill-posed problems, J. Soc. Math. 34 (3) (1986) 1656–1696.